*In partial fulfillment of the requirements for the M.S. degree in Chemistry from the University of Rochester. Present address: Research Laboratories, Eastman Kodak Company, Rochester, N. Y. 14650.
[1]J. L. J. Rosenfeld and J. Ross, J. Chem. Phys. **44,** 188 (1966).
[2]H. Y. Sun and J. Ross, J. Chem. Phys. **46,** 3306 (1967).
[3]C. Nyeland and J. Ross, J. Chem. Phys. **49,** 843 (1968).
[4]R. B. Bernstein and R. D. Levine, J. Chem. Phys. **49,** 3872 (1968); R. B. Bernstein, *Advances in Chemical Physics*, edited by J. Ross (Wiley, New York, 1966), Vol. 10.
[5]R. E. Roberts and J. Ross, J. Chem. Phys. **52,** 1464 (1970).
[6]J. Ross and E. F. Greene, *Molecular Beams and Reaction Kinetics*, edited by Ch. Schlier (Proceedings of the International School of Physics Enrico Fermi) (Academic, New York, 1970); D. Beck, E. F. Greene, and J. Ross, J. Chem. Phys. **37,** 2895 (1962).
[7]E. W. McDaniel, V. Cěrmák, A. Dalgarno, E. E. Ferguson, and L. Friedman, *Ion-Molecule Reactions* (Wiley-Interscience, New York, 1970), Chap. 3.3.C.
[8]L. L. Poulsen, J. Ross, and J. I. Steinfeld, J. Chem. Phys. **57,** 1592 (1972).
[9]T. Wu and T. Ohmura, *Quantum Theory of Scattering* (Prentice-Hall, Englewood Cliffs, N.J., 1962), Chap 1.A.
[10]Due to its energy dependence, the true optical potential is nonlocal. See discussions by D. A. Micha [J. Chem. Phys. **50,** 722 (1969)] and M. Rotenberg [Phys. Rev. A **4,** 220 (1971)].
[11]J. C. Y. Chen, *Advances in Radiation Chemistry*, edited by M. Burton and J. L. Magee (Wiley, New York, 1969), Vol. I.
[12]R. Marriott and D. A. Micha, Phys. Rev. **180,** 120 (1969).
[13]B. C. Eu, J. Chem. Phys. **52,** 3021 (1970).
[14]D. A. Micha and M. Rotenberg, Chem. Phys. Lett. **6,** 79 (1970).
[15]M. L. Goldberger and K. M. Watson, *Collision Theory* (Wiley, New York, 1964), pp. 882–898.
[16]M. E. Rose, *Elementary Theory of Angular Momentum* (Wiley, New York, 1957).
[17]F. T. Smith, J. Chem. Phys. **42,** 2419 (1965).
[18]W. H. Miller, J. Chem. Phys. **53,** 1949 (1970); J. Chem. Phys. **53,** 3578 (1970). For a similiar development see R. A. Marcus, Chem. Phys. Lett. **7,** 525 (1970); J. Chem. Phys. **54,** 3965 (1971).
[19]W. H. Miller, Chem. Phys. Lett. **7,** 431 (1970).
[20]W. H. Miller and T. F. George, J. Chem. Phys. **56,** 5637 (1972).
[21]W. H. Miller and T. F. George, J. Chem. Phys. **56,** 5668 (1972).
[22]T. F. George and W. H. Miller, J. Chem. Phys. **56,** 5722 (1972).
[23]T. F. George and W. H. Miller, J. Chem. Phys. **57,** 2458 (1972).
[24]D. Secrest and B. R. Johnson, J. Chem. Phys. **45,** 4556 (1966).
[25]In the actual computation of P_{semi} in Eq. (18) through the initial value representation (Ref. 18), the roots $\bar{q}_i^{(1)}$ and $\bar{q}_i^{(2)}$ are chosen such that $|\mathrm{Re}\bar{q}_i^{(1)} - \mathrm{Re}\bar{q}_i^{(2)}| \leq \pi$; e.g., where the value for $\mathrm{Re}\bar{q}_i^{(2)}$ at $E = 10$ is given as 6.23 in the table, the value used for $\mathrm{Re}\bar{q}_i^{(1)}$ is $6.23 - 2\pi$.
[26]R. A. Marcus, J. Chem. Phys. **57,** 4903 (1972).
[27]J. D. Doll and W. H. Miller, J. Chem. Phys. **57,** 5019 (1972).
[28]J. D. Doll, T. F. George, and W. H. Miller, J. Chem. Phys. **58,** 1343 (1973).
[29]J. D. Doll and T. F. George (unpublished).
[30]H. Feshbach, Ann. Phys. (N.Y.) **19,** 287 (1962). For discussion of energy-dependent, nonlocal potentials in molecular collisions, see R. D. Levine, *Quantum Mechanics of Molecular Rate Processes* (Oxford U. P., Cambridge, England, 1969), Chap. 3.
[31]P. Pechukas, Phys. Rev. **181,** 174 (1969).
[32]P. Pechukas and J. P. Davis, J. Chem. Phys. **56,** 4970 (1972).
[33]M. H. Mittleman and R. Pu, Phys. Rev. **126,** 370 (1962).

PHYSICAL REVIEW A VOLUME 8, NUMBER 1 JULY 1973

Excited-State Atomic-Hydrogen Population Resulting from 10-keV Proton and 20-keV H_2^+ Beams Colliding with a Magnesium Vapor Target*

L. D. Stewart† and H. K. Forsen‡
Department of Nuclear Engineering, The University of Wisconsin, Madison, Wisconsin 53706
(Received 30 November 1970; revised manuscript received 26 January 1973)

Investigations are made of the production of excited-state hydrogen neutrals using 10-keV proton or 20-keV H_2^+ beams and a magnesium vapor cell. Optical measurements are used to determine the population of the $n = 6$ level as a function of target thickness and to determine the relative populations for $3 \leq n \leq 8$. The cross section for capture into the $n = 6$ level for incident H_2^+ is found to be about equal to that for incident protons. An approximate $1/n^3$ dependence of the excited-state populations is found for $n \geq 6$ with an assumed $2l + 1$ weighted substate distribution.

I. INTRODUCTION

In some thermonuclear-fusion experiments, it is necessary to maximize the excited-state population of injected atomic-hydrogen beams in order to increase the trapped-particle density. An important aspect of this process is the ion-beam-neutralizer interaction. For the case of atomic hydrogen, it has been found that neutral-beam production may be enhanced by breakup plus neutralization of molecular ion (H_2^+) beams rather than by neutralization of protons.[1] The present work reports on an investigation of the relative excited-state production rates of protons and molecular ions for an atomic-beam energy of 10 keV and a magnesium neutralizer.

Excited-state production with protons incident on magnesium has been investigated for $n = 9$–16

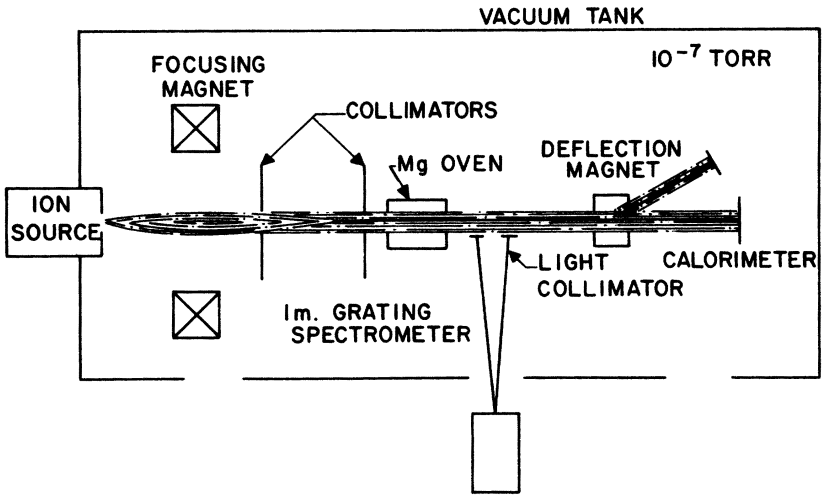

FIG. 1. Experimental apparatus.

with an electric-gap-ionization technique[2-4] and for $n=6$ by an optical technique.[5] Atoms with electrons in the $n=6$ state are not directly useful in thermonuclear experiments because the Lorentz fields created in most experiments are only sufficient to ionize states where $n \geq 10$. However, in most experiments the measured populations are found to scale as n^{-3} for the levels $n \simeq 9-16$, as is theoretically predicted.[6] Excited-state production with H_2^+ and H_3^+ ions incident on magnesium has been investigated using electric gap ionization.[4]

In the present experiments we have optically measured the intensity of the Balmer-series lines for transitions from the levels $3 \leq n \leq 8$ and have related intensities to excited-state-production cross sections by assuming various substate distributions. The measurement technique is similar to that used by Berkner *et al.*[5] for the level $n=6$. This method is more easily adapted to larger beams and can be applied during the injection of the neutral beam. It suffers in that some substate distribution must be assumed in order to relate intensities to populations and in that the intensities of the usable levels ($n \geq 9$) are not easily measured.

II. EXPERIMENTAL APPARATUS

The experimental apparatus is shown schematically in Fig. 1. The ion source is of the duoplasmatron type and is capable of operation in either a proton or a H_2^+ mode. A mass-dependent focusing system with collimators for intercepting the unwanted and defocused ions then further ensures the purity of the beam. An analysis of the ion components for both a 10-keV proton and a 20-keV H_2^+ beam reveals that both consist of greater than 95% of the desired ion species. The remainder of the proton beam is 10-keV H_2^+ and the remainder of the H_2^+ beam consists of about equal portions of 20-keV protons and 10-keV protons, with the latter coming from H_2^+ breakup on residual gas. These residual impurities are considered in the uncertainty analysis. Beams of 5-cm diam and either 7–10 mA of 10-keV protons or 10–20 mA of 20-keV H_2^+ are passed through a magnesium vapor cell, located about 100 cm from the source, and onto a target located 240 cm from the source.

The magnesium vapor cell is a Calrod-heated copper tube with tantalum end plates to prevent magnesium buildup.[7] Cell magnesium temperature is measured with two iron-constantin thermocouples. Magnesium line densities are determined by observing the neutral fraction of an emerging proton beam and then applying published ionization and neutralization cross sections.[8] An effective cell length is then determined by dividing the line density by the magnesium density inferred from the measured magnesium temperature and published vapor-pressure data.[9] The length determined in this manner is equal to the geometrical length (40 cm) within the uncertainty accrued from the uncertainty in the neutralization cross section.

Lines in the visible spectral region are observed with a 1.0-m Czerny-Turner spectrometer and an S-11 response photomultiplier tube. A grating grooved with 1180 lines/mm and blazed at 3000 Å is used, resulting in a system linear dispersion of 9.2 Å/mm. The beam is viewed through a Pyrex window with the entrance slit located 51 cm from the beam center. The segment of the beam viewed is defined by the 5.1-cm beam collimation and by slits. The slits are adjusted such that the length of the beam viewed is 4.8 cm and the viewed region begins 10.2 cm below the tantalum end plates of the magnesium cell.

Beam neutral fractions are determined by using a magnetic field transverse to the beam just below

the magnesium cell to deflect any charged particles remaining in the beam. Beam currents are determined by measuring the temperature rise and the flow rate of the target-cooling water.

Calibration of the optical system is done by observing the intensity of the $N_2^+(B\,^2\Sigma_u^+ \rightarrow X\,^2\Sigma_g^+)$ band at 3914 Å when passing a 20-keV proton beam through nitrogen at pressures of 1×10^{-4} to 1×10^{-5} torr. This method was selected because of the proximity of the 3914-Å band to the higher Balmer-series lines, because published absolute cross-section data are available for the production of this band,[10-14] and because proton bombardment of nitrogen is easily done in our system. The value selected for this cross section, $1.2\pm0.3\times10^{-16}$ cm^2, is that of Gardiner *et al.*[11] because of their apparent care in doing the measurement and the detail reported for their method.[15] The slit widths need to be sufficiently wide to pass all of the rotational structure which contributes to the N_2^+ band, and yet should be as narrow as possible to prevent impurity lines from interferring with the Balmer-line intensity measurements. A 26-Å spectral slit width was chosen after comparing a 1.6-Å scan with a published scan of the rotational structrue of the N_2^+ 3914-Å band.[12] Nitrogen pressures are determined by using a Bayard-Alpert ionization gauge. The effect of the H_1^0 component of the beam, which results from charge exchange with the nitrogen, is taken into account by using the published cross section for N_2^+ 3914-Å-band production by incident H_1^0.[11] The optical-system efficiency determined in this way showed day-to-day variations of 1% but no over-all change over a period of two months.

Balmer-series line intensities are normalized to 3914 Å by correcting for the differences in grating spectral response, for the differences in attenuation by the Pyrex viewing window, and for the response of the photomultiplier tube. These corrections are less than 15% on all lines except $n=3$. The line intensities are corrected for dark-current backgrounds and for zero-cell-density backgrounds arising from Balmer-series line production through neutralization of the ion beam by the residual gas in the beam drift region.

Reported measurements[5,11,16] indicate that both the 3914-Å band of N_2^+ and the $n=6$ line of the Balmer series are essentially unpolarized. No data could be found for the polarization of other Balmer-series lines and no polarization corrections are applied.

III. DATA ANALYSIS

In the process of neutralization of the ion beam within the charge-exchange cell, excited hydrogen atoms are produced. The decay of these beam atoms in the region viewed by the spectrometer provides Balmer-series line radiation. Determining the excited-state production rates can then be accomplished by first relating the transition rates in the viewed region $[N(H_n)]$ to the excited-state current leaving the cell (N_n^L) and then by relating N_n^L to the excited-state production rate in the cell (N_n^0).

The n-state atoms after leaving the cell are assumed to undergo no substate mixing. We are therefore concerned only with the substates which contribute directly to Balmer-series lines in the region beyond the cell. The lower level of Balmer-series transitions is $n'=2$ and has the substates $l'=0$ and 1. The selection rule $\Delta l=\pm1$ then means that only the substates $l=0,1$, and 2 contribute to Balmer-series transitions. Between the cell and the viewed region the effect of decay in the substates of concern will be given by the decay exponentials with each weighted by its relative population $[F_1(nl)]$:

$$\sum_{l=0}^{2} F_1(nl)\exp\left(\frac{-x_1A(nl)}{v}\right),$$

where x_1 is the distance between the cell and the viewed region and v is the beam-atom velocity. $A(nl)$ is the transition probability for the state nl and is given by the sum of the individual transition probabilities $[A(nl\rightarrow n'l')]$.

In the observation region, only those transitions resulting in a Balmer line need to be considered. The relevant transition probabilities are $A(nd\rightarrow 2p)$, $A(np\rightarrow 2s)$, and $A(ns\rightarrow 2p)$, with the transitions from each of the substates nl being a fraction $A(nl\rightarrow 2l')/A(nl)$ of the total transitions from state nl. The total number of transitions from the substate n will be one minus the decay exponential. Combining this we have

$$N(H_n)=N_n^L\sum_{l=0}^{2}F_1(nl)\exp\left(\frac{-x_1A(nl)}{v}\right)\frac{A(nl\rightarrow 2l')}{A(nl)}\times\left[1-\exp\left(\frac{-x_2A(nl)}{v}\right)\right], \quad (1)$$

where x_2 is the length of the viewed region.

The relationship between N_n^L and N_n^0 is obtained from the local-cell excited-state generation rate $[N_n(x)]$ due to n-state formation from H_2^+ ions and protons:

$$N_n(x)=\sigma_{p\rightarrow n}\rho I_p(x)+\sigma_{H_2^+\rightarrow n}\rho I_{H_2^+}(x), \quad (2)$$

where x is the penetration into the cell, $\sigma_{p\rightarrow n}$ and $\sigma_{H_2^+\rightarrow n}$ are the cross sections for n-state atom formation, $I_p(x)$ and $I_{H_2^+}(x)$ are the local proton and H_2^+ currents, and ρ is the cell magnesium line density.

In this analysis we neglect the contribution to the n-state population directly from neutrals. If the cross section for this process is small compared with the two excited-state-production cross sections considered, Eq. (2) will be a good assumption at the low cell densities where the cross-section determinations are made. This is because the neutral fractions at low cell densities are small. Assuming a constant cell density over the cell length (L), N_n^0 is now obtained by integrating $N_n(x)$ over the cell length

$$N_n^0 = \int_0^L N_n(x')\,dx' = \sigma_{p\to n}\rho\int_0^L I_p(x')\,dx' + \sigma_{H_2^+\to n}\rho\int_0^L I_{H_2^+}(x')\,dx' . \quad (3)$$

N_n^L is obtained by considering the decay of the n-state atoms in going from x to L with the velocity v. The decay will be given by the decay exponential using a total transition probability $A(n)$ obtained by weighting the substate transition probabilities $A(nl)$ with the relative populations $[F_2(nl)]$:

$$A(n) = \sum_{l=0}^{n-1} F_2(nl)\,A(nl) .$$

Integrating the decay of $N_n(x)$ over the cell length now gives N_n^L:

$$N_n^L = \int_0^L N_n(x')\exp\left(\frac{-(L-x')A(n)}{v}\right)dx' = \rho\int_0^L dx'\,[\sigma_{p\to n}I_p(x') + \sigma_{H_2^+\to n}I_{H_2^+}(x')] \times \exp\left(\frac{-(L-x')A(n)}{v}\right) . \quad (4)$$

The proton current $[I_p(x)]$ is obtained by considering that it is decreased by neutralization and increased by ionization of H_1^0 and by breakup of H_2^+:

$$dI_p(x) = -I_p(x)\sigma_{p\to H_1^0}\rho dx + I_{H_1^0}(x)\sigma_{H_1^0\to p}\rho\,dx + I_{H_2^+}(x)\sigma_{H_2^+\to p}\rho\,dx , \quad (5)$$

where $\sigma_{H_2^+\to p}$ is the cross section for proton production from H_2^+. The expression for the current $I_{H_2^+}(x)$ has the losses due to breakup and neutralization and the gain due to ionization of H_2^0:

$$dI_{H_2^+}(x) = \{-I_{H_2^+}(x)\,[\tfrac{1}{2}(\sigma_{H_2^+\to p} + \sigma_{H_2^+\to H_1^0}) + \sigma_{H_2^+\to H_2^0}] + I_{H_2^0}(x)\sigma_{H_2^0\to H_2^+}\}\rho\,dx , \quad (6)$$

where $\sigma_{H_2^+\to H_1^0}$ is the cross section for atom production from H_2^+, $\sigma_{H_2^+\to H_2^0}$ is the cross section for production of molecular neutrals from molecular ions, $\sigma_{H_2^0\to H_2^+}$ is the cross section for production of molecular ions from molecular neutrals, and $I_{H_2^0}(x)$ is the equivalent current of molecular neutrals.

Assuming no scattering losses in the cell, the incident nucleon current (I_0) is given by

$$I_0 = I_{H_1}(x) + I_p(x) + 2I_{H_2^+}(x) + 2I_{H_2^0}(x) , \quad (7)$$

where the factor of 2 in the H_2^+ term comes from an accounting of equivalent atomic units.

Simultaneous solution of Eqs. (1) and (3)–(7) now yields the cell excited-state production rate (N_n^0). Field-free transition probabilities as calculated by Hiskes and Tartar[17] are assumed and are given in Table I. The cross sections $\sigma_{p\to H_1^0}$ and $\sigma_{H_1^0\to p}$ are taken from Berkner *et al.*[8]; the cross sections $\sigma_{H_2^+\to p}$, $\sigma_{H_2^+\to H_1^0}$, $\sigma_{H_2^+\to H_1^0}$ are taken from Solov'ev *et al.*[4]; the cross sections $\sigma_{p\to n}$ and $\sigma_{H_2^+\to n}$ are to be results of this analysis, so initial estimates are made and an iterative procedure is used. No published values of $\sigma_{H_2^0\to H_2^+}$ were found, so extreme values of zero and infinity are used to establish limits on $\sigma_{H_2^+\to n}$. The extreme $\sigma_{H_2^0\to H_2^+}=0$ gives a lower limit for I_{H_1} and therefore an upper limit for $\sigma_{H_2^+\to n}$. The extreme $\sigma_{H_2^0\to H_2^+}=\infty$ gives an upper limit for I_{H_1} and therefore a lower limit for $\sigma_{H_2^+\to n}$.

These calculations are carried out using two

TABLE I. Balmer-series transition probabilities ($10^8\ s^{-1}$).

n	l	n'	l'	$A(nl\to n'l')$ Ref. 18
	0		1	0.0631
3	1	2	0	0.224
	2		1	0.646
	0		1	0.0258
4	1	2	0	0.0967
	2		1	0.206
	0		1	0.0129
5	1	2	0	0.0495
	2		1	0.0942
	0		1	0.007 35
6	1	2	0	0.0286
	2		1	0.0514
	0		1	0.004 59
7	1	2	0	0.0180
	2		1	0.0313
	0		1	0.003 05
8	1	2	0	0.0120
	2		1	0.0205
	0		1	0.002 14
9	1	2	0	0.008 44
	2		1	0.0142

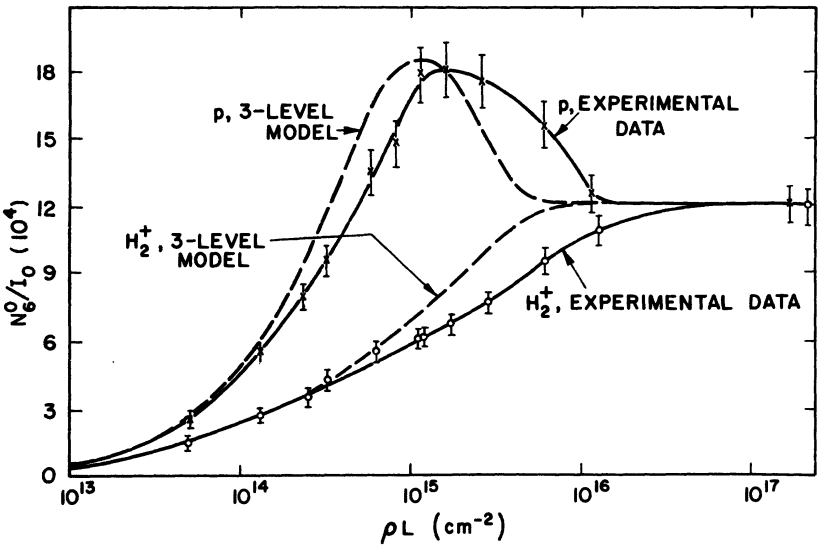

FIG. 2. Fraction of incoming nucleons excited to $n=6$ level as a function of the cell line density for incident 10-keV protons and 20-keV H_2^+. Also shown are results of three-level-model calculations.

different assumptions for the substate distribution. One is a distribution having all available substates for a given n equally populated, or a $(2l+1)$ weighting. Such a statistical distribution can be maintained by collisional and electric field mixing within the cell. This mixing process will be more effective as n increases because the energy differences between substates become smaller. The statistical distribution assumption enters our equations as

$$F_1(nl) = F_2(nl) = 2l+1/n^2 .$$

Another possible assumption is some given initial distribution undergoing decay but no mixing. For the levels $n=3$ and 4 and thin cells it has been found that the populations of the emerging beam are not statistical, but rather have a high population of the $l=0$ state.[18] The nonstatistical distributions of the $l=0$, 1, and 2 substates of the $n=3$ level for 10-keV protons incident on He, Ne, Ar, H_2, N_2, and O_2 from the data of Hughes *et al.*[19] were considered. No similar data for a magnesium target were found. All of these distributions produced a decrease of about the same magnitude in the excited-state cross sections over those calculated with the statistical distribution assumption. The O_2 distribution of 0.45, 0.35, and 0.15 for $l=0$, 1, and 2, respectively, results in the greatest decrease in the reported cross section, this being about 50% lower, and therefore it was used

TABLE II. Errors.

Source of error	Error in $\sigma_{p\to 6}=6.0\times10^{-18}$ cm^2 $+(\times10^{18}$ cm$^{-2})$	Error in $\sigma_{p\to 6}=6.0\times10^{-18}$ cm^2 $-(\times10^{18}$ cm$^{-2})$	Error in $\sigma_{H_2^+\to 6}=6.0\times10^{-18}$ cm^2 $+(\times10^{18}$ cm$^{-2})$	Error in $\sigma_{H_2^+\to 6}=6.0\times10^{-18}$ cm^2 $-(\times10^{18}$ cm$^{-2})$
±25% for published 3914-Å cross section	1.5	1.5	1.5	1.5
Uncertainty in pressure	0.49	0.49	0.49	0.49
Uncertainty in effective cell length	0.54	0.54	0.54	0.54
±20% for published $\sigma_{H_2\to}$	NA[a]	NA	<0.01	<0.01
±20% for published $\sigma_{H_2^+\to H_2^0}$	NA	NA	<0.01	<0.01
±20% for published $\sigma_{H_2^+\to p}$	NA	NA	<0.01	<0.01
Neglect of $\sigma_{H_1^0\to 6}$	0	0.15	0	0.15
$I_{H_1^0}(0)$	0.02	0.02	0.02	0.03
Beam-ion impurities	0.12	0	0	0.22
Total $X=\left(\sum x^2\right)^{1/2}$	1.67	1.67	1.67	1.69

[a] NA = does not apply.

for comparison in these calculations.

With an incident proton beam, $I_{H_2^+}(0)$ and $I_{H_2^+}(x)$ are zero and the equations become analytically solvable. Equations (3), (5), and (7) combine to give

$$N_n^0 = \frac{\sigma_{p\to n}}{\sigma_{H_1^0\to p}+\sigma_{p\to H_1^0}}\left(I_p(0) - \frac{I_0\sigma_{H_1^0\to p}}{\sigma_{H_1^0\to p}+\sigma_{p\to H_1^0}}\right) \times\{1-\exp[-(\sigma_{H_1^0\to p}+\sigma_{p\to H_1^0})\rho L]\}, \quad (8)$$

while Eqs. (4), (5), and (7) yield

$$N_n^L = \rho\sigma_{p\to n}\left(I_p(0) - \frac{I_0\sigma_{H_1^0\to p}}{\sigma_{H_1^0\to p}+\sigma_{p\to H_1^0}}\right) \times\left(\frac{\exp[-(\sigma_{H_1^0\to p}+\sigma_{p\to H_1^0})\rho L]-\exp[-LA(n)/v]}{[A(n)/v-\rho(\sigma_{H_1^0\to p}+\sigma_{p\to H_1^0})}\right) + \frac{\rho\sigma_{p\to n}\sigma_{H_1^0\to p}v}{(\sigma_{H_1^0\to p}+\sigma_{p\to H_1^0})A(n)}\{\exp[-LA(n)/v]-1\}. \quad (9)$$

IV. RESULTS

Figure 2 shows the fraction of the incoming nucleons which are converted to $n=6$ atoms, (N_6^0/I_0), obtained from the observed number of H_β transitions, the statistical substate distribution assumption, and Eqs. (3)–(7) as a function of the cell line density for incident 10-keV protons and 20-keV H_2^+. The cross sections for $n=6$ atom production are obtained from the linear relationship between N_6^0/I_0 and ρL at low cell densities. For an assumed statistical distribution the values are equal: $\sigma_{p\to 6}=\sigma_{H_2^+\to 6}=(6.0\times10^{-18}\ \text{cm}^2)\pm 30\%$. This indicates that the flux advantage possible in using molecular ion beams,[1] because of the Child-Langmuir law considerations and because each 20-keV H_2^+ is potentially two 10-keV H_1^0, is only available with thick targets when highly excited states are desired.

The cross-section uncertainties are shown in Table II and are dominated by the uncertainty in the N_2^+ 3914-Å-band-production cross section. Other sources of systematic error considered are the nitrogen pressure determination, effective cell-length determination, uncertainties in the published H_2^+ cross sections, neglect of excited-state production from neutrals, and the effect of ion and neutral impurities in the incident beam. The effect of a preferential loss of the excited-state atoms, because they are skimmed off as they diverge within the cell,[20] is estimated to be small and no error was assigned. Considered as sources of random error are the beam-current measurement, the optics calibration, and the line-intensity measurement. The error bars shown in Fig. 2 are for random error only.

The $n=6$ population collisional-loss cross section ($\sigma_{6\to}$) and the cross section for producing $n=6$ atoms in beam magnesium atom collisions ($\sigma_{H_1^0\to 6}$) are estimated by fitting a three-level model[21] to the proton data. The three levels are considered as currents of protons (I_p), ground-state atoms ($I_{H_1^0}$), and $n=6$ atoms (N_6^0). The appropriate equation is then

$$dN_6^0 = [I_p(x)\sigma_{p\to 6}+I_{H_1^0}(x)\sigma_{H_1^0\to 6}-N_6^0(x)\sigma_{6\to}]\rho\,dx. \quad (10)$$

The solution to this equation is fitted to the proton data of Fig. 2 by varying $\sigma_{H_1^0\to 6}$ and $\sigma_{6\to}$ to get simultaneously the correct asymptotic population and as nearly as possible the correct peak population and its corresponding line density. The resulting cross sections are $\sigma_{H_1^0\to 6}\approx 1.5\times10^{-18}$ cm^2 and $\sigma_{6\to}\approx 1.4\times10^{-15}$ cm^2. Although these values are well determined by this procedure, no combination of values makes the three-level-model curve fit within the error bars of more than a few points. These values can therefore at most be considered

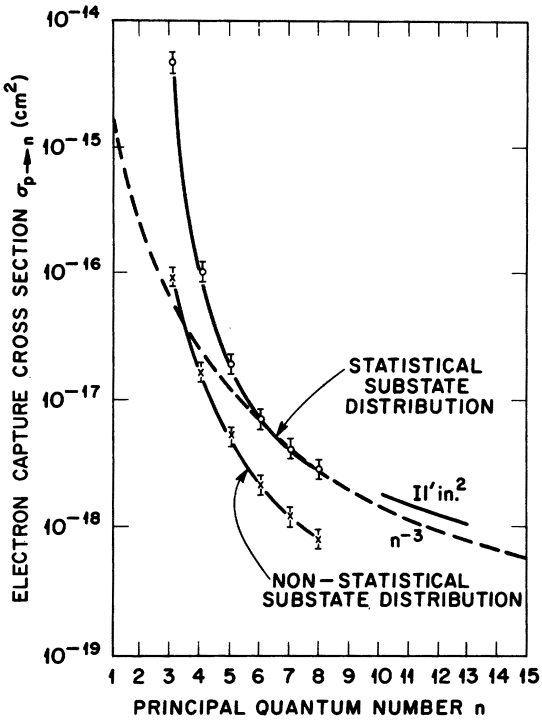

FIG. 3. Experimental cross section for electron capture into various n levels for incident 10-keV protons using statistical and nonstatistical weightings of substates. Results of Il'in *et al.* (Ref. 2) are shown for higher levels. The theoretical n^{-3} distribution is shown normalized to the total capture cross section at $n=1$.

estimates and the three-level model cannot be used as a basis for assigning uncertainties. An H_2^+ level is now added to the model, which adds the term $I_{H_2^+}\sigma_{H_2^+\to 6}\rho\, dx$ to the right-hand side of Eq. (10). With all cross sections determined above, the fit of the H_2^+ curve shown in Fig. 2 is obtained.

Our cross section $\sigma_{p\to 6} = (6.0\times10^{-18}\ \text{cm}^2)\pm 30\%$ agrees with the value reported by Berkner *et al.*[5] of $8.7\pm 3.1\times10^{-18}$ cm^2 for the same statistical distribution assumption. Our estimated values $\sigma_{H_1^0\to 6}\approx 1.5\times10^{-18}$ cm^2 and $\sigma_{6\to}\approx 1.4\times10^{-15}$ cm^2 can be compared to their estimates of $\sigma_{H_1^0\to 6}\approx 5\times10^{-19}$ cm^2 and $\sigma_{6\to}\approx 1.7\times10^{-15}$ cm^2.

The low-density cross-section determinations were done for proton beams and the levels $3\leq n\leq 8$. A spectral slit width of 3.5 Å is used to resolve higher Balmer lines from impurity lines and the results normalized to the $n=6$ cross section reported above. The $n=9$ line could not be resolved from an impurity line. These results are shown in Fig. 3 for both the statistical and the nonstatistical distribution assumptions. The error bars shown are random errors only. Also shown are the electric-field-ionization data of Il'in *et al.*[2] for $10\leq n\leq 13$ and a dashed $1/n^3$ plot normalized to the total caputure cross section $\sigma_{p\to H_1^0}$.

The cross section $\sigma_{p\to 3}$ calculated with the statistical distribution assumption is higher than the total neutralization cross section ($\sigma_{p\to H_1^0}$) so this assumption cannot hold for $n=3$. A peak in $\sigma_{p\to n}$ at $n=2$, as predicted by Hiskes,[22] would fit well with the nonstatistical distribution data. On the other hand, a $1/n^3$ distribution is predicted[6] for higher n, and the statistical distribution data follow this curve at higher n but the nonstatistical distribution data do not. Considering these things and the fact that energy differences between substates decrease with increasing n, it would seem plausible that as n is increased above 3 the substate distribution goes from one similar to that of Hughes *et al.*[19] to a statistical distribution at $n=6$.

Electric-field measurements of Il'in *et al.*[2] for $10\leq n\leq 13$ result in $n^3\sigma_{p\to n} = 2\times10^{-15}$ cm^2, as shown in Fig. 3. Our measurements for $n=6$, 7, and 8 yield $n^3\sigma_{p\to n} = 1.3\times10^{-15}$ cm^2.

V. CONCLUSIONS

The excited-state populations of 10-keV atomic-hydrogen beams resulting from neutralization of a 10-keV proton beam and from dissociation and neutralization of a 20-keV H_2^+ beam are measured and analyzed. The results show that the cross sections for the two processes are the same when considering only the number of incident charged particles. Therefore the potential increase in neutral-beam currents, because H_2^+ ions can become two hydrogen atoms, carries over to excited-state production only for thick targets. An approximate n^{-3} dependence of the excited-state population is found if a statistical distribution is assumed for $n\geq 6$.

*Work supported in part by the National Science Foundation.
†Present address: Oak Ridge National Laboratory, Oak Ridge, Tenn. 37830.
‡Present address: Exxon Nuclear Co., Inc.

[1]J. E. Osher, Lawrence Radiation Laboratory Report No. UCRL 73412, 1971 (unpublished).
[2]R. N. Il'in, V. A. Oparin, E. S. Solov'ev, and N. V. Fedorenko, Zh. Eksp. Teor. Fiz. Pis'ma Red. **2**, 310 (1965) [JETP Lett. **2**, 197 (1965)].
[3]V. A. Oparin, R. N. Il'in, and E. S. Solov'ev, Zh. Eksp. Teor. Fiz. **52**, 369 (1967) [Sov. Phys.-JETP **25**, 240 (1967)].
[4]E. S. Solov'ev, R. N. Il'in, V. A. Oparin, and N. V. Fedorenko, Zh. Eksp. Teor. Fiz. **53**, 1933 (1967) [Sov. Phys.-JETP **26**, 1097 (1968)].
[5]K. H. Berkner, W. S. Cooper III, S. N. Kaplan, and R. V. Pyle, Phys. Rev. **182**, 103 (1969).
[6]S. T. Butler and R. M. May, Phys. Rev. **137**, A10 (1965).
[7]R. C. Davis, R. R. Hall, G. G. Kelly, O. B. Morgan, and R. F. Stratton, Oak Ridge National Laboratory Report No. ORNL-4063, 1966 (unpublished).
[8]K. H. Berkner, R. V. Pyle, and J. W. Stearns, Phys. Rev. **178**, 248 (1969).
[9]R. E. Honig, RCA Rev. (Radio Corp. Am.) **18**, 195 (1937).
[10]F. J. deHeer and J. F. M. Aarts, Physica (Utr.) **48**, 620 (1970).
[11]H. A. B. Gardiner, W. R. Pendleton, Jr., J. J. Merrill, and D. J. Baker, Phys. Rev. **188**, 257 (1969).
[12]D. J. Baker, H. A. B. Gardiner, and J. J. Merrill, J. Chim. Phys. **64**, 63 (1967).
[13]J. L. Philpot and R. H. Hughes, Phys. Rev. **133**, A107 (1964).
[14]W. F. Sheridan, O. Oldenberg, and N. P. Carlton, in *Proceedings of the Second International Conference of Physics of Electronic and Atomic Collisions: Abstracts of Papers* (Benjamin, New York, 1961), p. 159.
[15]H. A. B. Gardiner, J. J. Merrill, W. R. Pendleton, Jr., and D. J. Baker, Appl. Opt. **8**, 799 (1969).
[16]E. W. Thomas, G. D. Bent, and J. L. Edwards, Phys. Rev. **165**, 32 (1968).
[17]J. R. Hiskes and C. B. Tarter, Lawrence Radiation Laboratory Report No. UCRL-7088, Rev. I, 1964 (unpublished).
[18]J. L. Edwards and E. W. Thomas, Georgia Institute of Technology Report No. ORO-2591-47, 1970 (unpublished).
[19]R. H. Hughes, C. A. Stigers, B. M. Doughty, and E. D. Stokes, Phys. Rev. A **1**, 1424 (1970).
[20]J. Kingdon, M. F. Payne, and A. C. Riviere, J. Phys. B **3**, 552 (1970).
[21]K. H. Berkner, L. Kay, and A. C. Riviere, Nucl. Fusion **7**, 29 (1967).
[22]J. R. Hiskes, Phys. Rev. **180**, 146 (1969).